Near-field dynamics of ultrashort pulsed Bessel beams in media with Kerr nonlinearity

P. Polesana,[1,*] A. Dubietis,[1,†] M. A. Porras,[2] E. Kučinskas,[1] D. Faccio,[3] A. Couairon,[4] and P. Di Trapani[1,3]
[1]*Department of Quantum Electronics, Vilnius University, Saulėtekio Ave. 9, bldg.3, LT-10222 Vilnius, Lithuania*
[2]*Departamento de Fisica Aplicada, Universidad Politecnica de Madrid, Rios Rosas 21, E-28003 Madrid, Spain*
[3]*Dipartimento di Fisica, Università dell'Insubria, via Vallegio, 11 22100 Como, Italy*
[4]*Centre de Physique Theorique, Ecole Polytechnique, CNRS UMR 7644, F-91128 Palaiseau, France*
(Received 10 April 2006; published 22 May 2006)

The near-field dynamics of a femtosecond Bessel beam propagating in a Kerr nonlinear medium (fused silica) is investigated both numerically and experimentally. We demonstrate that the input Bessel beam experiences strong nonlinear reshaping. Due to the combined action of self-focusing and nonlinear losses the reshaped beam exhibits a radial compression and reduced visibility of the Bessel oscillations. Moreover, we show that the reshaping process starts from the intense central core and gradually replaces the Bessel beam profile during propagation, highlighting the conical geometry of the energy flow.

DOI: 10.1103/PhysRevE.73.056612 PACS number(s): 42.65.Tg, 42.65.Jx, 42.65.Re

Bessel beams (BBs) are peculiar light beams that result from the interference of plane waves whose wave vectors lie on a conical surface. The near-field, i.e., the transverse amplitude profile of a BB takes the form of a Bessel J_0 function, with an intense central peak of width down to a few wavelengths. A distinctive feature of BBs is that power flows along the conical surface and not along the propagation axis as in conventional Gaussian beams. The central peak is apparently diffraction-free and is surrounded by slowly decaying tails in the form of concentric rings that contain the major part of the beam power (each ring carries an equal amount of power). Due to the finite extent of the beam limited by the particular geometry of any practical realization, the propagation of experimentally generated BBs is thus diffraction-free over finite distances only, although larger by orders of magnitude than those achievable by conventional laser beams with the same spot diameter [1].

As proposed in 1987 [2], BBs have found a range of applications, such as micromanipulation of particles in multiple planes realizing three-dimensional optical tweezers [3] and optical levitation [4]; these beams possess a good potential for free-space optical interconnects [5] and electron acceleration [6], to mention a few. Specific properties (nondiffracting propagation, self-reconstruction) due to the conical nature of BBs have been exploited in various fields of nonlinear optics, where practical benefits are expected. In particular, BBs have been shown to produce efficient Raman radiation [7], diffraction-limited parametric superfluorescence [8], continuous plasma channels [9], high-order harmonic generation [10], and excitation of fluorescence channels via multiphoton absorption [11]. In device-oriented applications, BBs were used for material modification [12] and in optical microlitography [13].

To date, most studies devoted to the nonlinear propagation of BBs mainly concern the transformations occurring in the far field of the fluence distribution. In particular, in media with Kerr nonlinearity, the appearance of an axial component and the generation of additional rings in the far field have been demonstrated with picosecond laser pulses [14,15]. A complete near-field characterization of the nonlinear dynamics of BBs should provide relevant complementary information. So far, radial compression/expansion of the BB has been predicted to occur from numerical simulations in the case of focusing/defocusing nonlinearity [16]. However, near-field measurements of the nonlinear dynamics are still missing for initial BBs.

In this paper, we report on a near-field observation of the evolution of an intense ultrashort pulsed BB undergoing Kerr self-focusing and nonlinear losses (NLL) in fused silica. Under frequently encountered operating conditions, the input BB experiences a progressive reshaping, evidenced by radial compression and contrast attenuation, that reduces visibility of the Bessel oscillations. The observed reshaping dynamics is driven by the combined action of self-focusing and NLL occurring in the intense central core of the BB. In particular, NLL induce unbalancing between the inward and outward Hankel components [17,18], which constitute the input BB.

In the experiment we used the laser pulse delivered by a Nd:glass laser system (TWINKLE, Light Conversion Ltd). The ultrashort pulsed BB was generated by launching a 200 fs, 1.4 mm full width at half-maximum (FWHM), 527 nm wavelength Gaussian beam into a BK7 glass axicon of 2° 50′ base angle. The axicon generated BB had a Bessel zone of about 50 mm length, and the maximum intensity of the central spot was reached 19 mm after the axicon. The measured width of the central spot was 7 μm FWHM. We used several fused silica samples of different lengths (2, 3, 5, and 8 mm) placed with the input facet at the location of this maximum intensity. The energy of the input BB was set to 27 μJ, so as to generate a stable axial component in the far field, thus ensuring a nonlinear propagation regime in the sample. The output facet of the sample was imaged onto a CCD camera (COHU, 10 bit dynamic range, pixel dimension 9.9 μm with Spiricon frame grabber) with a 45 mm focal length lens, corresponding to a 10.8× magnification (for a resolution of 0.92 μm/pixel). For comparison, we also recorded the fluence profiles in the case of a low-energy (<1 μJ) input BB propagating linearly.

The results are reported in Fig. 1. The solid curves repre-

*Permanent address: Dipartimento di Fisica Università dell'Insubria, via Vallegio, 11 22100 Como, Italy.
†Author to whom all correspondence should be addressed: Email address: audrius.dubietis@ff.vu.lt

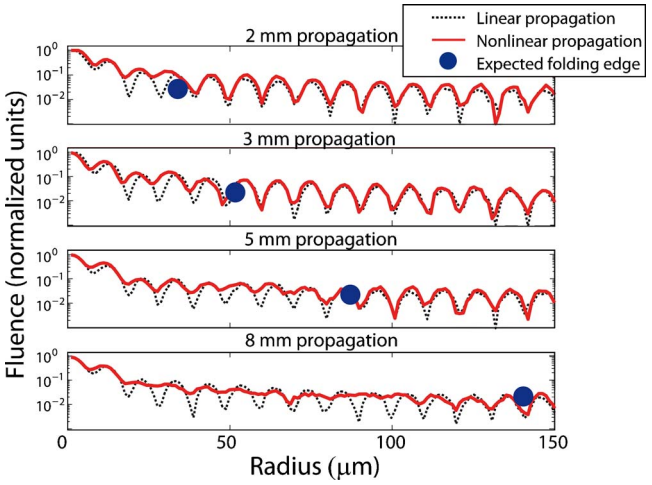

FIG. 1. (Color online) Experimental fluence profiles (logarithmic scale of normalized units) showing the progressive reshaping of a BB: the solid curve shows the reshaped BB at the output facet of each sample of different length (2, 3, 5, and 8 mm); the dotted curve shows the fluence profile of a BB linearly propagated through the same samples. The bold dot is the predicted folding edge.

sent the evolution of the fluence profile in the nonlinear regime, while the dotted curves correspond to the linear propagation of the low-energy BB. The fluence profile is reshaped within a circular region of increasing radius, while out of this region it remains almost indistinguishable from the linearly propagated BB. The folding edge between the reshaped and the nonreshaped part (shown by the bold dots) is found to be well described by a radius θz, where $\theta = 1.01°$ is the cone angle of the input BB (in the medium, i.e., taking into account the refraction index) and z is the propagation distance. Figure 2 shows a magnification of the reshaped portion of the near field at $z=5$ mm. The beam profile is characterized

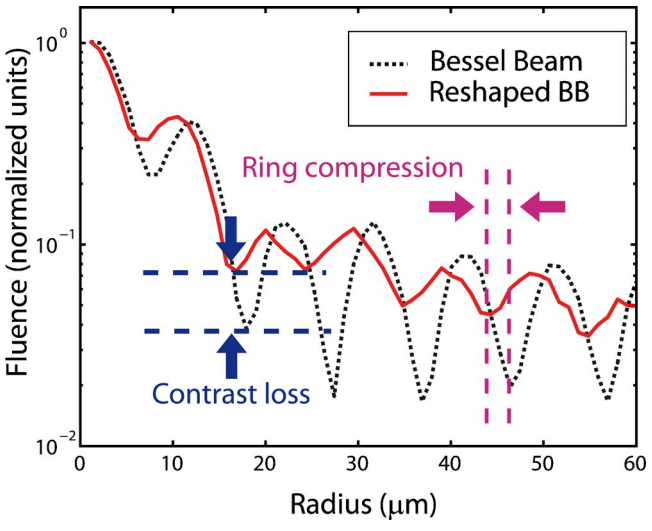

FIG. 2. (Color online) Magnification of the fluence profile (logarithmic scale of normalized units) of the reshaped BB (solid line) after the nonlinear propagation through a 5-mm-long fused silica sample, compared with the linearly propagated BB (dotted line) through the same sample.

by ring compression, which we attribute to Kerr nonlinearity, and by contrast attenuation, arising from NLL.

The key features of the experimentally observed nonlinear dynamics were reproduced in detail by means of numerical simulations with our code described in Ref. [19]. The code solves the nonlinear equation for the envelope $\mathcal{E}(r,t,z)$ of the laser field with central frequency ω_0 and accounts for diffraction, dispersion, self-focusing, and NLL,

$$\hat{U}\frac{\partial \hat{\mathcal{E}}}{\partial z} = i\left[\frac{\nabla_\perp^2}{2k_0} + \frac{k_0}{2}\left(\frac{k^2}{k_0^2} - \hat{U}^2\right)\right]\hat{\mathcal{E}} + \hat{\mathcal{F}}\{N(\mathcal{E})\}, \tag{1}$$

where $\hat{\mathcal{E}}(r,\omega,z) = \hat{\mathcal{F}}\{\mathcal{E}(r,t,z)\}$ ($\hat{\mathcal{F}}$ denotes the Fourier transform for the time/frequency domains) and $X_{\mathrm{FT}}\{N(\mathcal{E})\}$ denotes the Fourier transform of the nonlinear terms. Here $k(\omega) \equiv n(\omega)\omega/c$ denotes the wave number of the Fourier components, $n(\omega)$ is the linear refraction index, $k_0 \equiv \omega_0 n(\omega_0)/c$, $n(\omega_0) = 1.46$, $\hat{U}(\omega) \equiv 1 + (\omega - \omega_0)/k_0 v_g$, and $v_g \equiv \partial\omega/\partial k|_{\omega_0}$ is the group velocity of the input pulse. In this way, high-order dispersive terms are also accounted for, even if they do not play any important role under our operating conditions. The nonlinear term includes self-focusing and NLL,

$$N(\mathcal{E}) = i\frac{\omega_0}{c}n_2 T^2|\mathcal{E}|^2\mathcal{E} - T\frac{\beta_K}{2}|\mathcal{E}|^{2K-2}\mathcal{E}. \tag{2}$$

The nonlinear refractive index of fused silica $n_2 = 3.5 \times 10^{-16}$ cm^2/W was taken from Ref. [20]. With the band gap of fused silica being 7.5 eV [21], NLL are expected to be a four-photon absorption process, and the multiphoton absorption coefficient β_K ($K=4$) was computed from Keldysh's formulation [22] ($\beta_4 = 1.2 \times 10^{-38}$ cm^5/W^3 with an electron-hole reduced mass of 1) in the multiphoton ionization limit. This is fully justified by the fact that the intensity never exceeds $I = 10^{12}$ W/cm^2 in our calculations. The operator $T \equiv 1 + \frac{i}{\omega_0}\frac{\partial}{\partial t}$ is responsible for pulse self-steepening and optical shocks, which were found from our simulations to be negligible effects. We modeled the propagation of a Gaussian-apodized pulsed BB with input-pulse parameters corresponding to the experiment, namely wavelength 527 nm, pulse duration 200 fs, energy 27 μJ, central peak FWHM 7 μm, and 1.4 mm FWHM Gaussian apodization.

The results of numerical simulations are presented in Fig. 3, which compares the reshaped fluence profiles (solid curves) with linearly propagated BBs (dotted curves) at the same propagation distances as in the experiment. The general trend is similar to that shown by the experimental results in Fig. 1, yet the numerical results allowed us to better capture the fine details of the transition between the internal (nonlinear) and the external (linear) regions, which does not exhibit abrupt changes in contrast and oscillatory ring position.

Our experimental and numerical results show that the input BB experiences a gradual reshaping that starts from the intense core of the BB and expands as a circle of linearly increasing radius with propagation distance, as dictated by the conical geometry of the energy flow. Within this circle, the input BB undergoes radial compression and contrast attenuation indicated by reduced visibility of the Bessel oscillations. For the different sample lengths considered in the

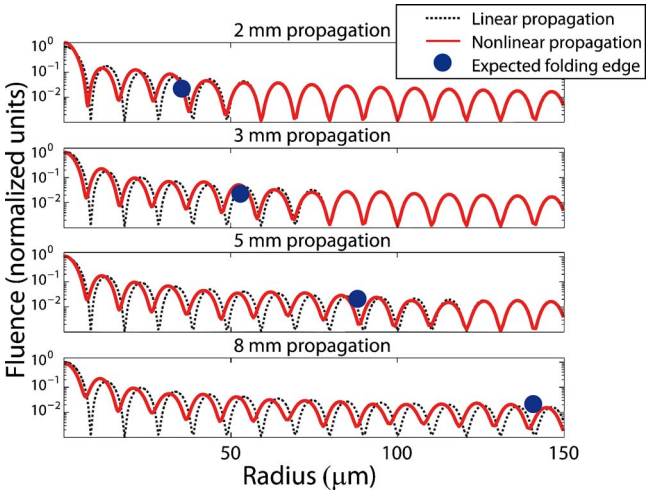

FIG. 3. (Color online) Fluence profiles from numerical simulations (logarithmic scale of normalized units) of the progressive reshaping of an input BB.

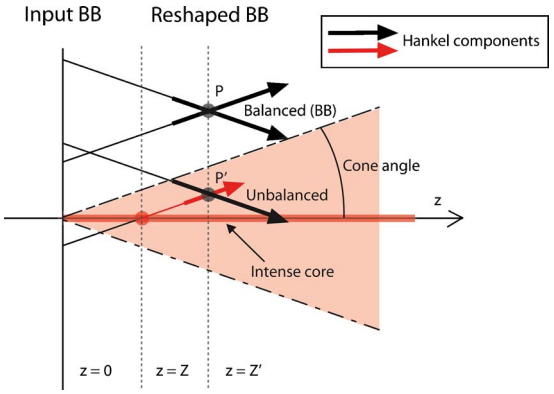

FIG. 4. (Color online) Graphical explanation of the progressive reshaping of the BB during propagation in Kerr nonlinear medium.

experiment, the intersections between the Bessel cone angle (1.01° in our fused silica samples) and the output facets of the samples lie on circles of radii 35, 52, 88, and 141 μm marked by the bold dots in Figs. 1 and 3. These marks separate the zone of nonlinear propagation (inner) from that featured by the linear regime (outer). The profiles corresponding to the intense (solid curves) and weak (dotted curves) fields coincide in the outer region, indicating that the tails of the field propagated linearly up to this distance without experiencing the reshaping triggered by the intense central core. In contrast, in the inner region, the reshaped BB is established.

The good agreement between the experimental and numerical results suggests an interpretation of the reshaping dynamics in terms of Kerr- and NLL-induced unbalance between the two Hankel components which constitute the input BB. To this end, it is worth mentioning that the power flux in a BB can be represented as the sum of the flux from two Hankel waves, one carrying energy toward the central peak and the other flushing it outward [17,18],

$$\mathcal{E} = \alpha_{\text{in}} H_0^{(1)} + \alpha_{\text{out}} H_0^{(2)}, \tag{3}$$

where α_{in} and α_{out} denote the complex amplitudes of inward and outward Hankel components, respectively. Note that α_{in} and α_{out} are equal for a BB.

Figure 4 explains the main features of the reshaping dynamics of a BB launched in a nonlinear Kerr medium. Since nonlinear effects occur mainly in the intense central core, the field at any point P outside the Bessel cone centered on the central peak (depicted by dot-dashed lines) is the result of the superposition of the "fresh" inward and outward Hankel components, hence a BB. However, at any point P' inside the cone, a single Hankel component passed through the intense core, where it experienced nonlinear absorption and a nonlinear phase shift due to the Kerr effect. The field at point P' is then the superposition of these two unbalanced Hankel beams. The resulting profile can still be described by Eq. (3), but with $\alpha_{\text{in}} \neq \alpha_{\text{out}}$. The most evident effect of amplitude unbalancing due to NLL ($|\alpha_{\text{in}}| \neq |\alpha_{\text{out}}|$) is the creation of a net inward radial power that attenuates the contrast $C = 2|\alpha_{\text{in}}||\alpha_{\text{out}}|/(|\alpha_{\text{in}}|^2 + |\alpha_{\text{out}}|^2)$ of the Bessel oscillations, reaching $C=0$ (no oscillations) in a pure Hankel beam, while $C=1$ for a balanced BB. The nonlinear phase shift due to Kerr nonlinearity leads to a phase shift $\arg(\alpha_{\text{in}}) - \arg(\alpha_{\text{out}})$ between the interfering Hankel beams, which manifests itself as a radial compression of the maxima and minima of the intensity profile [23]. Thus the near-field reshaping dynamics of a BB launched in a nonlinear Kerr medium can be verified by the appearance of ring compression and contrast attenuation, which are the signatures of Kerr self-focusing and NNL, respectively. These findings suggest that the near-field dynamics of the input BB can be understood as a gradual evolution toward the nonlinear unbalanced Bessel beam, in which unbalancing of the inward and outward conical energy fluxes acts as a refilling mechanism that compensates for NLL in the central core of the beam.

In conclusion, investigation of the nonlinear propagation of a high-power femtosecond BB launched in a Kerr medium (fused silica) suggests that the observed near-field reshaping dynamics is linked to the spontaneous formation of the nonlinear unbalanced Bessel beam, which is a stationary and weakly localized solution of the nonlinear Schrödinger equation in the presence of self-focusing and NLL [24]. The main features of the nonlinear unbalanced Bessel beam, e.g., ring compression due to self-focusing and contrast attenuation due to NLL, were recorded. Moreover, the observed reshaping dynamics indicate that the nonlinear unbalanced Bessel beam is formed from the intense central core and progressively replaces the BB profile during propagation following the conical geometry of the energy flow.

ACKNOWLEDGMENTS

P.P. acknowledges the support from Sixth EU Framework Programme Contract No. MEST-CF-2004-008048 (ATLAS). M.A.P. and P.D.T. acknowledge the support from Accion Integrada Hispano-Italiana H12004-0078. P.D.T. acknowledges support from Marie Curie Chair project STELLA, Contract No. MEXC-CT-2005–025710.

[1] D. McGloin and K. Dholakia, Contemp. Phys. **41**, 15 (2005).
[2] J. Durnin, J. J. Miceli, and J. H. Eberly, Phys. Rev. Lett. **58**, 1499 (1987).
[3] V. Garcez-Chavez, D. McGloin, H. Melville, W. Sibbett, and K. Dholakia, Nature (London) **419**, 145 (2002).
[4] V. Garces-Chavez, D. Roskey, M. D. Summers, H. Melville, D. McGloin, E. M. Wright, and K. Dholakia, Appl. Phys. Lett. **85**, 4001 (2004).
[5] N. Al-Ababneh and M. Testorf, Opt. Commun. **242**, 393 (2004).
[6] S. Liu, H. Guo, H. Tang, and M. Liu, Phys. Lett. A **324**, 104 (2004).
[7] I. Golub, Opt. Lett. **20**, 1847 (1995).
[8] A. Piskarskas, V. Smilgevičius, and A. Stabinis, Appl. Opt. **36**, 7779 (1997).
[9] J. Fan, E. Parra, and H. M. Milchberg, Phys. Rev. Lett. **84**, 3085 (2000).
[10] C. Altucci, R. Bruzzese, C. de Lisio, M. Nisoli, E. Priori, S. Stagira, M. Pascolini, L. Poletto, P. Villoresi, V. Tosa, and K. Midorikawa, Phys. Rev. A **68**, 033806 (2003).
[11] P. Polesana, D. Faccio, P. Di Trapani, A. Dubietis, A. Piskarskas, A. Couairon, and M. A. Porras, Opt. Express **13**, 6160 (2005).
[12] J. Amako, D. Sawaki, and E. Fujii, J. Opt. Soc. Am. B **20**, 2562 (2003).
[13] M. Erdelyi, Z. L. Horvath, G. Szabo, Zs. Bor, F. K. Tittel, J. R. Cavallaro, and M. C. Smayling, J. Vac. Sci. Technol. B **15**, 287 (1997).
[14] R. Gadonas, V. Jarutis, R. Paškauskas, V. Smilgevičius, A. Stabinis, and V. Vaičaitis, Opt. Commun. **196**, 309 (2001).
[15] V. Pyragaitė, K. Regelskis, V. Smilgevičius, and A. Stabinis, Opt. Commun. **257**, 139 (2006).
[16] P. Johannisson, D. Anderson, M. Lisak, and M. Marklund, Opt. Commun. **222**, 107 (2003).
[17] S. Chavez-Cerda, G. S. McDonald, and G. H. C. New, Opt. Commun. **123**, 225 (1996).
[18] J. Salo, J. Fagerholm, A. T. Friberg, and M. M. Salomaa, Phys. Rev. E **62**, 4261 (2000).
[19] A. Couairon, E. Gaižauskas, D. Faccio, A. Dubietis, and P. Di Trapani, Phys. Rev. E **73**, 016608 (2006).
[20] R. DeSalvo, A. A. Said, D. J. Hagan, E. W. Van Stryland, and M. Sheik-Bahae, IEEE J. Quantum Electron. **32**, 1324 (1996).
[21] A. Brodeur and S. L. Chin, J. Opt. Soc. Am. B **16**, 637 (1999).
[22] A. M. Perelomov, V. S. Popov, and M. V. Terent'ev, Sov. Phys. JETP **23**, 924 (1966).
[23] M. A. Porras, A. Parola, and P. Di Trapani, J. Opt. Soc. Am. B **22**, 1406 (2005).
[24] M. A. Porras, A. Parola, D. Faccio, A. Dubietis, and P. Di Trapani, Phys. Rev. Lett. **93**, 153902 (2004).